

RESEARCH PAPER

Preparation and Characterization of Multiwalled Carbon Nanotubes-Polythiophene Nanocomposites and its Gas Sensitivity Study at Room Temperature

Sanjay Gorakh Bachhav and Dilip Ramsing Patil *

Nanomaterial research Laboratory, R. C. Patel A C S College, Shirpur, India

ARTICLE INFO

Article History:

Received 14 July 2017

Accepted 21 September 2017

Published 01 October 2017

Keywords:

Carbon Nanotubes

Conducting Polymer

Gas Sensitivity

In-situ Polymerization

Nanocomposite

ABSTRACT

The nanocomposites of polythiophene and carboxylated multiwalled carbon nanotubes (MWCNTs) were synthesized by in-situ chemical oxidative polymerization method using anhydrous ferric chloride (FeCl_3) as an oxidant. The MWCNTs functionalized and ultrasonicated to obtain uniform dispersion within the polythiophene matrix. Field emission scanning electron microscopy was used to characterize the morphology of the nanocomposite. X-Ray diffraction, Fourier Transform Infrared Spectroscopy, Raman spectroscopy, and thermogravimetric analysis were used to characterize the synthesized MWCNT-polythiophene nanocomposites. It was found that in-situ polymerized polythiophene layer matrix was formed on carboxylated MWCNT and there was uniform dispersion of MWCNTs within the polythiophene matrix with significant interaction between polythiophene and MWCNTs. The sensitivity response of the prepared MWCNT-polythiophene nanocomposite sensors was studied in using Ammonia gas. The synergistic effects of the polythiophene-coated MWCNTs improve the gas sensing properties. Results showed that the sensitivity increased with ammonia concentration and it is also affected by the MWCNT content in polythiophene matrix. Furthermore, the sensor in pellet form reported here is robust, cost effective, and relatively stable at room temperature.

How to cite this article

Bachhav SG, Patil DR. Preparation and Characterization of Multiwalled Carbon Nanotubes-Polythiophene Nanocomposites and its Gas Sensitivity Study at Room Temperature. J Nanostruct, 2017; 7(4):247-257.

INTRODUCTION

Ammonia (NH_3) sensing is very crucial factor to both environment as well as the medical field, as it is one of the most harmful pollutant gases present in the atmosphere produced by human activity and industrial process. Its exposure to human affects health significantly [1]. In addition, the presence of ammonia in exhaled human breath beyond certain level can be regarded as symptomatic of several diseases related to liver and kidneys [2].

Conducting polymers are widely used in sensing materials due to its cost effectiveness, high sensitivity, fast response, and room temperature operations. Today, a vast number

of conducting polymers and their derivatives are known. Compared to the inorganic counterpart, conducting polymers are more sensitive and selective by virtue of their chemical and structural diversity. Among several conducting polymers, polyaniline, polypyrrole and polythiophene has been commonly employed in gas sensor applications due to its excellent electrical properties, easy synthesis, good environmental stability, and cost effectiveness [3-5]. Carbon nanotubes (CNTs) discovered by S. Iijima in 1991 have been great interest, both from a fundamental point of view and promising applications in the field of nanoscience and nanotechnology [6,7].

* Corresponding Author Email: dr.drpatil@gmail.com

Polythiophene (PTh) is one of the most promising conducting polymer and extensively studied for their extraordinary properties such as high stability of doped and undoped states, ease of structural modification and controllable electrochemical behavior [8]. Its excellent properties lead to improved performance in numerous potential applications in many fields [9-11]. However, the electrical conductivity of PTh is quite low due to wide energy gap and lack of electrons in its anti-bonding orbit [12]. To expand the application scope of PTh, the doped PTh and its composite with other nanoparticles are researched extensively [4, 13, 14]. The pure PTh when combined with different inorganic materials to form nanocomposites, it exhibits several exceptional properties and becomes useful in several technological applications. Kong et al. [4] and Xu et al [13] prepared polythiophene-SnO₂ nanocomposite gas sensor for NO_x detection at low temperature. Guo et al. [15] synthesized PTh-WO₃ nanocomposite for NO₂ sensing and showed that the hybrid material exhibited high response and good stability at low temperature.

The studies on polymer based nanocomposites showed that the properties of PTh can also be dramatically improved by incorporating CNTs into PTh matrix. The electrical conductivity of conducting polymers is known to be greatly influenced by the chemical insaturation surrounding the polymer backbone, besides the presence of favorable conformation of the side chains. However, the incorporation of CNT into polymer matrix can provide a conductive path at relatively low CNT content because of high aspect ratio, large specific area and metallic characteristics [16, 17], consequently improves the transport properties of polymer. Therefore the use of MWCNT-polymer composite in various applications such as optoelectronic devices, supercapacitors, sensors and so forth becomes prominent.

The gas sensors developed so far were in thin/thick film and pellet form. Thin/thick film gas sensors required the use of substrate for deposition of sensing material with some particular technique [18-21]. However, the pellet form of gas sensor does not require any substrate and time consuming deposition technique. Therefore, pelletized gas sensors are cost effective, robust, and reasonably sensitive. Sing et al. [22] designed and fabricated pelletized

LPG sensor using iron-antimonate nanostructured material. Barkade et al. [23] developed PTh based composite sensor in pellet form for systematic study of LPG sensing. Venkatesan et al. [24] reported the study of conducting polymer-based nanomaterial pelletized sensor for NH₃ sensing. Yun et al. [25] prepared PANI-MWCNT composite by applying simple oxyflurination method to control the morphology and discussed its effect on NH₃ sensing of composite pellet sensors.

In the present work, polythiophene-coated multiwalled carbon nanotube composites were synthesized by simple, cost-effective in situ oxidative polymerization method. The gas sensors were prepared in pellet form, which is be robust, cheap, and reasonably sensitive to ammonia vapor sensing. The gas sensitive characteristics of composite for different MWCNT content and over wide range of NH₃ vapor concentration were investigated at room temperature. The effect of humidity, long term stability and selectivity was also studied.

MATERIALS AND METHODS

Chemicals

MWCNTs and Triton X 100 are received from sigma Aldrich. The Thiophene monomer used was acquired from SDFC (Mumbai). Anhydrous ferric chloride (FeCl₃) was used as oxidizing agents acquired from Merck India. All these reagents used were analytical grade.

Material synthesis

Surface modification and functionalization of MWCNTs were made by using acid boiling reflux treatment. MWCNTs were suspended in H₂SO₄ and HNO₃ in a ratio of 3:1v/v to introduce the functional group into the surface of MWCNTs. The suspension was refluxed with vigorous stirring at 80°C for 12 h. After cooling to the room temperature, the mixture was filtered with filter paper. The filtrated solid was then washed thoroughly with DI water until neutral pH, and then washed with ethanol. The collected product was dried in oven at 60°C for 12 h. This product is referred to as functionalized MWCNTs [26].

The MWCNT-PTh composites were synthesized by in-situ chemical oxidative polymerization process using anhydrous FeCl₃ as an oxidant. In a typical synthesis experiment, a certain amount of f-MWCNT was added to 60 ml CHCl₃ and 50 μl of Triton X 100 was added as a surfactant to this

mixture so as to disperse the f-MWCNTs in CHCl_3 . The solution then ultrasonicated over 1 h to form well dispersed MWCNT suspension. A required amount of thiophene monomer (0.25M) was added into this MWCNT suspension with constant stirring followed by sonication for 10 min. A required amount of Anhydrous FeCl_3 added in 60 ml CHCl_3 to make 0.75M FeCl_3 solution and added to the Thiophene-MWCNT mixture. The mole ratio of FeCl_3 /Thiophene monomer was 3:1. The stirring was continued for 3 hrs and then kept standing the solution for 12 h at room temperature. During the synthesis procedure, the color of the composite suspension changed from black to dark red, which indicated the successful formation of PTh over the surface of MWCNTs. The polymerized solution was filtered and washed several times with methanol. The final product was dried at 70°C for 12 h to obtain MWCNT-PTH nanocomposite.

A series of six MWCNT-PTH nanocomposite samples with 0.25 wt%, 0.5 wt. %, 1 wt.%, 2 wt.%, 4 wt.%, and 8 wt.% of MWCNT contents in PTh matrix keeping its concentration fixed were prepared. The pristine PTh sample was also synthesized using the similar method given above except use of MWCNTs.

Characterizations

The morphology of the synthesized nanocomposites was studied using Hitachi S4800 Type-II field emission scanning electron microscopy (FESEM). X-ray diffraction (XRD) patterns were performed on a Bruker D8 Advance diffractometer with $\text{Cu K}\alpha$ radiation. Raman spectra were recorded at room temperature on JYHoriba HR800 Raman spectrometer employing 488 nm Argon laser beam. Fourier transform infrared (FT-IR) spectra were recorded on a Shimadzu IR Affinity spectrophotometer with KBr pellets to ensure functional groups. Thermogravimetric analysis (TGA) was performed using a Perkin Elmer 4000 Thermogravimetric analyzer in temperature range from room temperature to 700°C with heating rate of 20°C/min under N_2 flow to study the thermal degradation of the samples.

Sample preparation and Gas testing

The pure PTh and MWCNT-PTH nanocomposite powder was pressed into pellets of diameter 15 mm and thickness ~ 5 mm by hydraulic press (Kimaya, Pune) under identical conditions. The pellets to be serving as gas sensors, the electrical

contacts are made at a distance about 12 mm with the help of silver paste on one of the surface of the pellet. The gas sensing test was carried out in an indigenous designed instrument and fabricated by Subhadra Scientific, Pune. The detailed experimental setup of gas sensing apparatus is described elsewhere [27].

RESULTS AND DISCUSSIONS

Characterization of MWCNT-Pth nanocomposite

The morphology of f-MWCNTs, pure PTh and MWCNT-PTH nanocomposites shown by FE-SEM images in Fig. 1. The intermingle ropes with smooth surface of f-MWCNTs with diameter about 10 nm and lengths up to few μm was observed in FE-SEM image shown in Fig. 1(a). The pure PTh exhibit flake-like structure with ~50 nm thickness as seen in Fig. 1(b). For MWCNT-PTH samples, the coating of PTh was observed on the surface of MWCNT leading to rope like morphology (Fig. 1(c) and 1(f)). The results of FESEM images clearly indicates that the presence of MWCNT into PTh matrix significantly influence the morphology of the PTh around the MWCNT [28]. The PTh deposited MWCNTs containing 2 wt. % of MWCNT were observed to be more thicker as compared with MWCNT-PTH sample with 4 wt. %. This is obvious because of decrease in PTh content as MWCNT content increased.

The XRD pattern of pure PTh, MWCNT and MWCNT-PTH are shown in Fig. 2. For pure PTh, a broad, amorphous diffraction peak appeared at approximately $2\theta = 15\text{-}30^\circ$, attributed to the existence of polythiophene in amorphous form [23]. The XRD spectra for f-MWCNT show the presence of two peaks at $2\theta = 26^\circ$ and 43° assigned to (002) and (100) diffraction planes of carbon atom, respectively, in good agreement with that reported earlier [29]. The MWCNT-PTH exhibit little shifting the position of PTh diffraction peak with the addition of MWCNT content, indicating the physical wrapping of the PTh over the surface of MWCNTs. The XRD results clearly indicate that the PTh in composite is also amorphous, and the addition of MWCNT do not alter the amorphous state of PTh [30].

Raman spectroscopy was carried out to ensure the interaction between PTh and MWCNTs. The typical Raman spectra MWCNT, PTh and MWCNT-PTH composites are shown in Fig. 3. The Raman spectrum of the carboxylated MWCNTs demonstrated two prominent characteristics

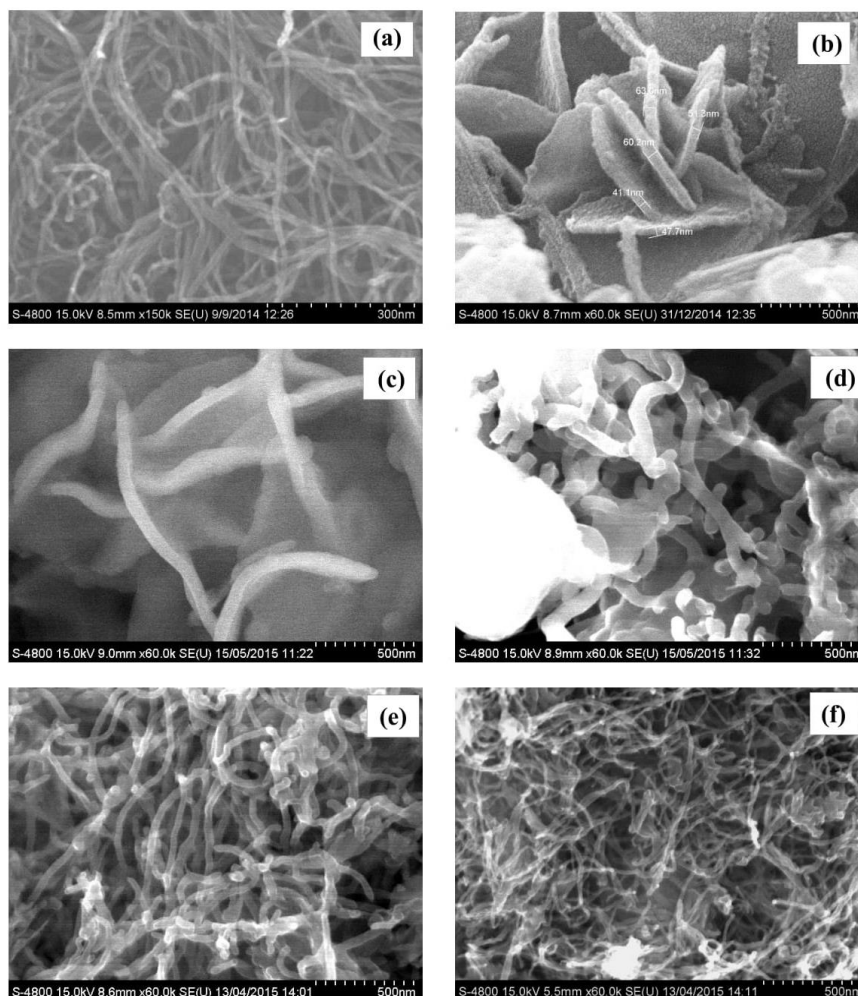


Fig. 1. FE-SEM images of (a) f-MWCNT (b) pure PTh and MWCNT-PTh nanocomposites at (c) 0.5 wt. %, (d) 1 wt. %, (e) 2 wt. %, and (f) 4 wt. % MWCNT content.

peaks: D band (1350 cm^{-1}) and G band (1580 cm^{-1}). The D band represents a disorder induced feature and is usually due to presence of amorphous disordered carbon structure of CNTs [31] and G band represents stretching mode of C-C bond [32]. The Raman spectra of pure PTh show two main peaks, where the first prominent peak appeared within $1400\text{--}1500\text{ cm}^{-1}$ corresponds to C=C stretching region, which is symmetric in phase vibration of thiophene ring. The second small peak observed in the range $1030\text{--}1070\text{ cm}^{-1}$ corresponds to C-C stretching along with C-H wagging component. This vibrational feature confirmed that the π electrons in PTh are confined within each thiophene ring. The Raman spectra of MWCNT-PTh composites are modified and

include the features of both, PTh and MWCNT demonstrating that the MWCNT serve as the core in the formation of MWCNT-PTh nanotubular composites [33].

The FT-IR spectra recorded for MWCNT, PTh and its nanocomposites in the $400\text{--}4000\text{ cm}^{-1}$ range is shown in Fig. 4. In the FT-IR spectrum of functionalized MWCNT, the peaks at 1390 and 1535 cm^{-1} attributed to bending vibration of O-H group and carbonyl, respectively. The small intense peak at $\sim 1700\text{ cm}^{-1}$ corresponded to the C=O stretching vibration mode, representing the formation of the carboxylic groups and a broad peak at 3460 cm^{-1} characteristic of an O-H stretch was observed due to alcoholic or phenolic carboxylic groups. These results specified that

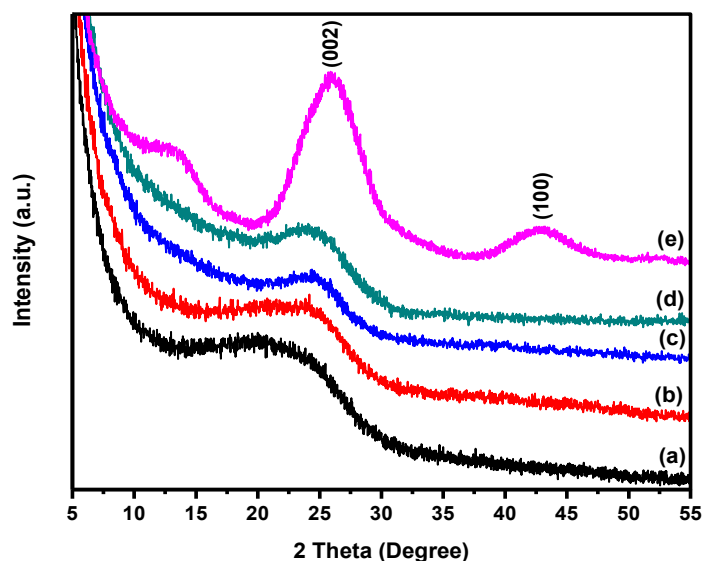


Fig. 2. XRD patterns of (a) pure PTh, MWCNT-PTh nanocomposites at (b) 1 wt. %, (c) 2 wt. %, (d) 4 wt. % MWCNT content and (e) f-MWCNT.

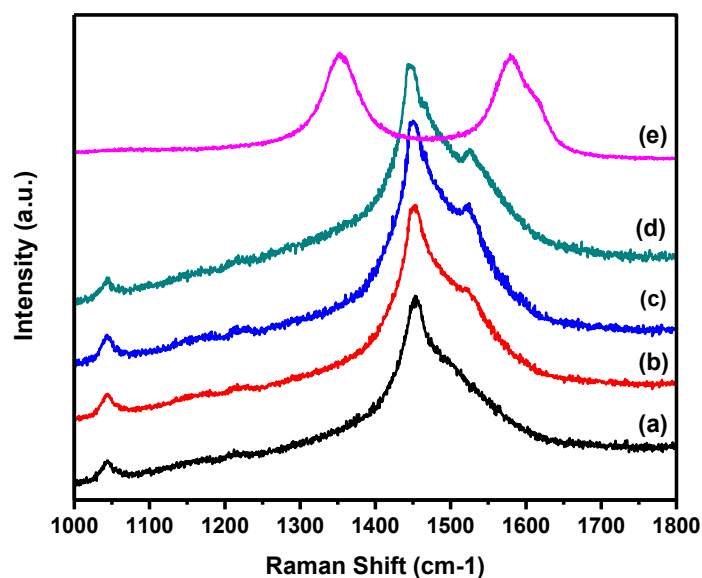


Fig. 3. Raman spectroscopy of (a) pure PTh, MWCNT-PTh nanocomposites at (b) 1 wt. %, (c) 2 wt. %, (d) 4 wt. % MWCNT content and (e) f-MWCNT.

the MWCNTs had been successfully oxidized into carboxylated carbon nanotubes [34]. The range of 400-2000 cm^{-1} represents the fingerprint region of PTh. The high intense characteristics peak at 788 cm^{-1} in the spectra of pure PTh is due to C-H out of plane deformation mode of thiophene ring arise from the polymerization of thiophene monomer [5]. The peak at 696 cm^{-1} has been identified for C-S bending mode indicating the presence of thiophene monomer [33]. The peak at 1640 and

1402 cm^{-1} corresponds to C=C asymmetric and symmetric stretching vibrations of thiophene ring respectively [35]. The peak at 1215 cm^{-1} is assigned to C-C stretching vibration while the peak at 1031 cm^{-1} is assigned to C-H in plane bending [36]. The peak at 468 cm^{-1} corresponds to C-S-C ring deformation [37]. The MWCNT-PTh samples exhibit almost the same number of peaks and positions of the peaks within the range of 400-2000 cm^{-1} [38]. The peak intensity of 788 cm^{-1} reduced

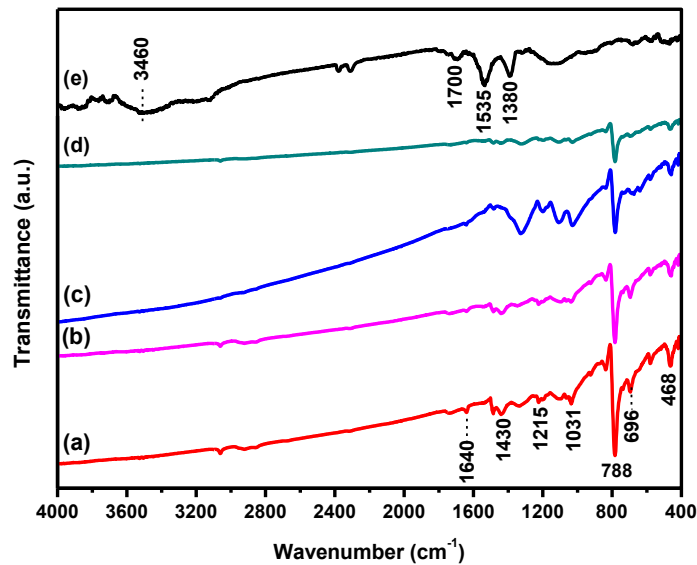


Fig. 4. FT-IR spectrum of (a) pure PTh, MWCNT-PTh nanocomposites at (b) 1 wt. %, (c) 2 wt. %, (d) 4 wt. % MWCNT and (e) f-MWCNT

in the MWCNT-PTH composites is due to the interfacial entrapment between MWCNT surface and PTh [39]. There are several low intensity peaks present in the range of 2800-3000 cm^{-1} , which can be attributed to the C-H stretching vibrations.

Thermogravimetric analyzer (TGA) measurements were carried out to investigate the effect of incorporation of functionalized carbonylated MWCNT on thermal stability of MWCNT-PTH. The results of MWCNT-PTH nanocomposites along with

pure PTh and f-MWCNT for comparison are shown in Fig. 5. It is observed that the pure PTh was stable up to 375 $^{\circ}\text{C}$ and rapid mass loss occurred thereafter, and loses 55% mass loss at 500 $^{\circ}\text{C}$. The f-MWCNTs are comparatively more stable and showing no dramatic decomposition, with a 15 % mass loss occurred in observed temperature range [29]. This loss may be due to the decomposition of functional groups (such as C=C and COOH) present in MWCNTs. As compared to pure PTh,

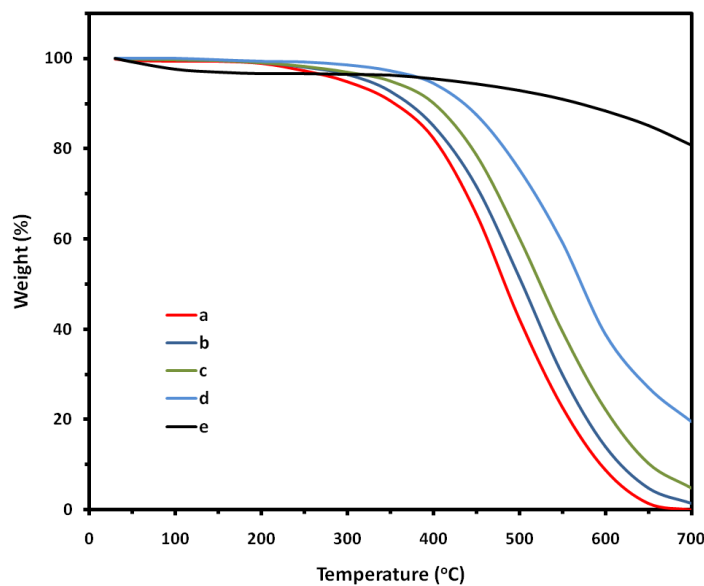


Fig. 5. TGA curves of (a) pure PTh, MWCNT-PTh nanocomposites at different MWCNTs contents of (b) 1 wt.% (c) 2 wt.% (d) 4 wt.% and (e) f-MWCNT

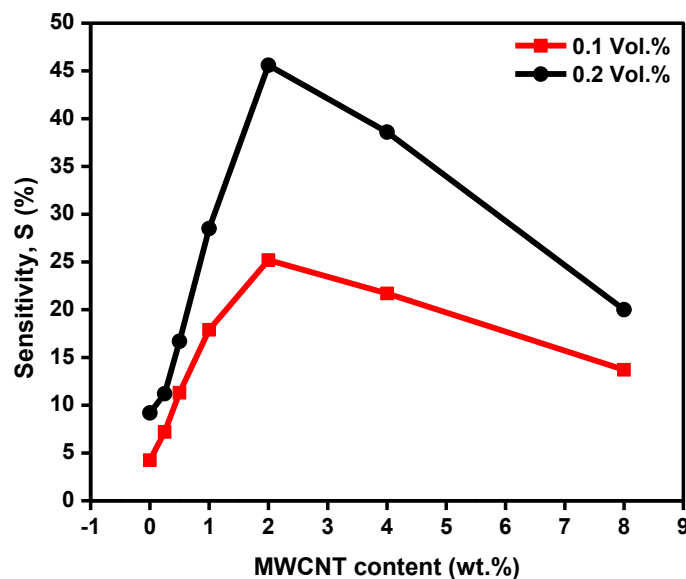


Fig. 6. Response of MWCNT-PTH nanocomposite with different MWCNT content exposed to 0.1 vol. % and 0.2 vol. % NH_3 concentrations at room temperature.

the MWCNT-PTH nanocomposite samples showed slower decomposition. The thermal stability of MWCNT-PTH samples increased with the increase of the MWCNTs content in PTH. This indicates that the addition of the carboxylated MWCNT had improved the thermal stability of MWCNT-PTH nanocomposites.

Sensing mechanism and Gas sensing test

The electrical resistance of PTH and MWCNT-PTH sensors increased when they are exposed to NH_3 gas. The change in electrical resistance of these sensors is attributed to the charge transfer mechanism between NH_3 gas molecules and MWCNT-PTH surface. Such p-type behavior was also observed in PTH-based [4, 15, 23] and MWCNT-based gas sensors [18, 40], where PTH and MWCNT behave as p-type semiconductors. This implies that, the MWCNT-PTH composite also act as a p-type semiconductor. The adsorption of NH_3 gas molecules on PTH and MWCNT-PTH nanocomposite cause net charge transfer from NH_3 molecules to sensors leading to the localization of polarons in PTH and its composite sensors. This results in increase in resistance.

The sensing characteristics of all prepared nanocomposite sensors including pure PTH for 0.1 vol % and 0.2 vol.% NH_3 concentration at room temperature is shown in Fig. 6. It can be observed that the response of composite to NH_3 gas increased initially as MWCNT content

increased up to 2 wt. %, and decreased afterward for further increase in MWCNT. The MWCNT-PTH sensor synthesized for 2 wt. % MWCNT show the highest response (45.6 %) at room temperature. Therefore it is predicted that the sensitivity of composite sensor is greatly influenced by variation in the MWCNT content, because of the content of CNT strongly affecting the morphology and the electrical property of the Polymer-CNT composites [41-43]. The increase in sensitivity with increase in MWCNT content is attributed to increase of surface area of composite material, providing more active sites for adsorption of NH_3 gas molecules and thus increase in sensitivity. However, further increase in MWCNT content makes the composite electrically shorted, thereby increasing the percolation effect by highly conductive carbon nanotubes [44]. Also, the conductivity of the composite is dominated by the metallic CNTs. This suggests that both these phenomenon could be responsible for decrease in the composite sensor response.

The variation of response of PTH and MWCNT-PTH sensors at room temperature to different concentration (0.02-0.2 vol.%) of NH_3 is shown in Fig. 7. The graph revealed that the sensitivity of sensors linearly increased with NH_3 concentration indicating that the gas response is function of gas concentration. It was observed that MWCNT-PTH composite exhibits higher response as compared to pure PTH. The enhanced sensitivity response of MWCNT-PTH composite is due to the synergistic

effect of pure PTh and due to f-MWCNTs. The sensitivity of composite sensor increased from 10.4 % to 45.6 % over 0.02-0.2 vol. % concentration range of NH_3 , while for pure PTh it increased only 1.7 % to 9.2 % for the same range. This is because the sensitivity of sensor depends on the removal of adsorbed oxygen molecules by reaction of target gas and generation of electrons. For a smaller concentration of gas exposed on fixed surface area of sensor, lower surface reaction was occurred due to lower coverage of gas. An increase in gas

concentration raises the surface reaction due to larger surface coverage [45].

The room temperature transient gas response curve of the composite sensor (2 wt.%) to 0.2 vol.% NH_3 concentration is shown in Fig. 8. A rapid increase in resistance is observed initially, as adsorption process taking place very fast at initial stage and afterward, it become slower near the equilibrium. After reaching the resistance to equilibrium, the NH_3 gas inside the chamber was withdrawn using vacuum pump and dry nitrogen

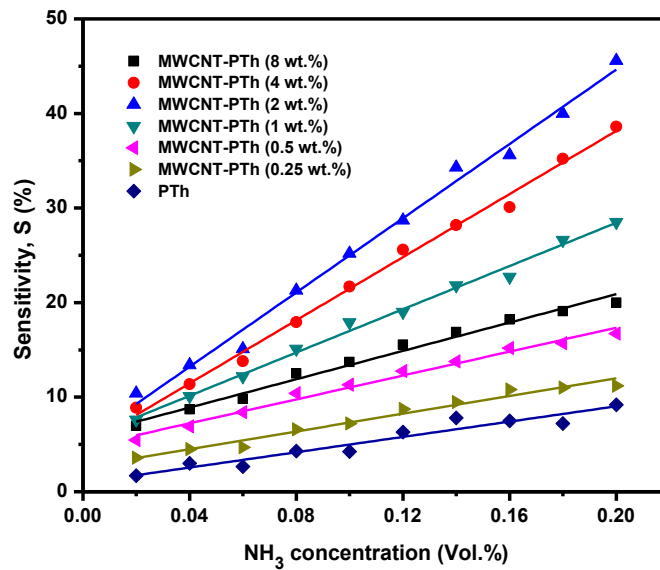


Fig. 7. Response of PTh and MWCNT-PTh sensors as a function of NH_3 concentration

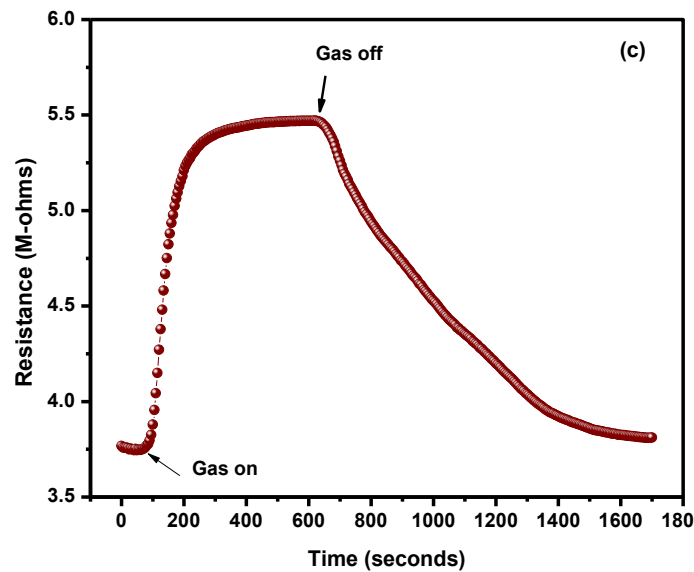


Fig. 8. Response-recovery of MWCNT-PTh (2 wt. %) sensors towards 0.2 vol. % NH_3

(N₂) is injected into the glass chamber to recover the resistance to its original value. A gradual decrease in resistance was then observed and approaching towards the baseline resistance value (R₀). It is observed that the response and recovery times of nanocomposite sample are 102 s and 470 s respectively.

Stability is the very important parameter to be considered for the evaluation of reliability of sensor. In order to study the stability, MWCNT-PTH (2 wt.%) sensors were exposed to 0.2 vol.% of NH₃ gas at room temperature and the response was

recorded for 40 days at an interval of 4 days. The result is represented in Fig. 9. It can be observed from the response curve that the composite sensors exhibit fairly constant response over the duration of 40 days. This suggests that the MWCNT-PTH sensors exhibit long term stability.

The selectivity of MWCNT-PTH composite sensor was also tested for Liquefied petroleum gas (LPG), and vapors of volatile organic compounds (VOCs) such as Ethanol, Methanol, Acetone and Chloroform at the same concentration. The response is represented in Fig. 10. The MWCNT-

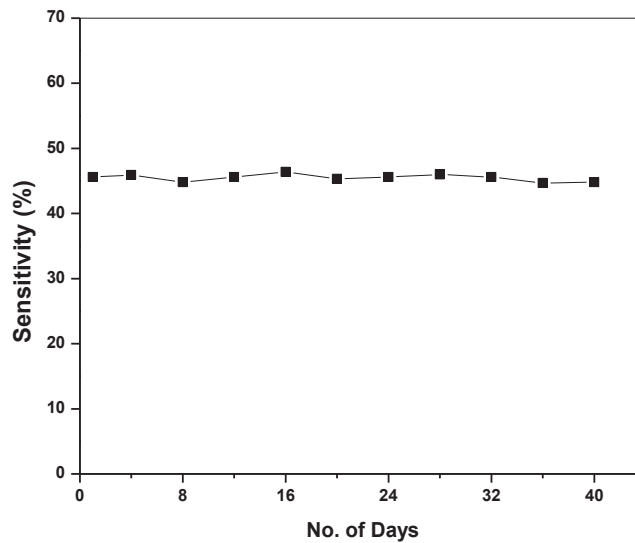


Fig. 9. Stability of MWCNT-PTH (2 wt.%) nanocomposite sensor towards 0.2 vol.% NH₃ concentration

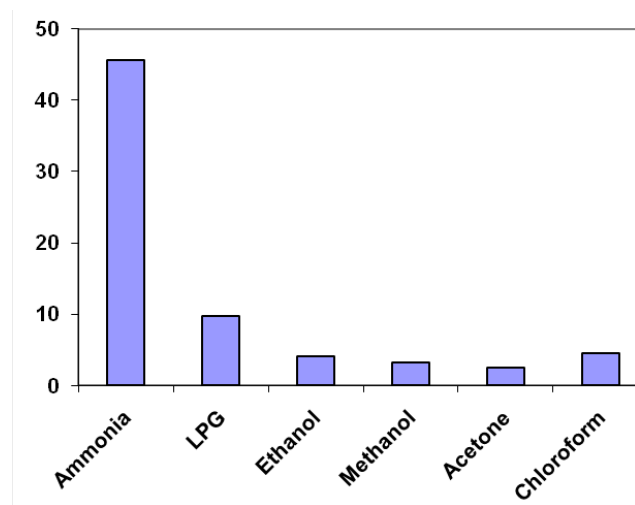


Fig.10. Selectivity of MWCNT-PTH (2 wt.%) nanocomposite sensor towards 0.2 vol.% NH₃ concentration

PTH sensor showed very high response as compared to other gases and was found to be highly selective towards NH_3 . The composite pellet sensor showed small (<5%) response to Ethanol, Methanol, Acetone and Chloroform vapors, while showed comparatively higher response (~10%) to LPG. The stability and selectivity tests indicate that the fabricated MWCNT-PTH composite pellet sensor is reliable and shows potential application in the field of gas sensing.

CONCLUSIONS

A series of MWCNT-PTH nanocomposite were synthesized by in-situ oxidation polymerization of thiophene monomer and MWCNT with different content. FE-SEM images confirmed that PTH layer was successfully formed on the surface of MWCNTs. XRD, Raman, FT-IR and TGA characterization of composites revealed the occurred entrapment between the MWCNT and PTH. The MWCNT-PTH composites indicated improved thermal stability compared to pure PTH. The MWCNT-PTH nanocomposites pellet sensors shown good sensitivity to NH_3 gas at room temperature. The content of MWCNT in the PTH significantly affects the sensitivity towards NH_3 . The most sensitive MWCNT-PTH nanocomposites sensor to NH_3 gas obtained with 2 wt % MWCNT content and showed good stability and selectivity towards NH_3 .

ACKNOWLEDGEMENTS

The authors are grateful to University Grant Commission, New Delhi for financial support through Minor Research Project scheme no. F. 47-809/13 (WRO). The authors are also thankful to 'UGC-DAE Consortium for Scientific Research Centre, Indore' for providing the characterization facilities and the Management of 'R.C. Patel Educational Trust, Shirpur' for their continuous encouragement and support.

CONFLICT OF INTEREST

The authors declare that there are no conflicts of interest regarding the publication of this manuscript.

REFERENCES

1. Timmer B, Olthuis W, Van Den Berg A. Ammonia sensors and their applications-a review. *Sens Actuators B*, 2005; 107(2); 666-677.
2. Risby T, Solga S. Current status of clinical breath analysis. *Appl Phys B*, 2006; 85(2-3); 421-426.
3. Abdulla S, Mathew T, Pullithadathil B. Highly sensitive, room temperature gas sensor based on polyaniline-multiwalled carbon nanotubes (PANI/MWCNTs) nanocomposite for trace-level ammonia detection. *Sens Actuators B*, 2015; 221; 1523-1534.
4. Kong F, Wang Y, Zhang J, Xia H, Zhu B, Wang Y, et al. The preparation and gas sensitivity study of polythiophene/ SnO_2 composites. *Mater Sci Eng B*, 2008; 150(1); 6-11.
5. Bai S, Zhang K, Sun J, Zhang D, Luo R, Li D, et al. Polythiophene- WO_3 hybrid architectures for low-temperature H_2S detection. *Sens Actuators B*, 2014; 197; 142-148.
6. Malekshahi Byranvand M. Recent development of carbon nanotubes materials as counter electrode for dye-sensitized solar cells. *J Nanostruct*, 2016; 6(1); 1-16.
7. Jalajardi R, Ghanbari D. Microwave Synthesis and Magnetic Investigation of CuFe_2O_4 Nanoparticles and Poly Styrene-Carbon Nanotubes Composites. *J Nanostruct*, 2016; 6(4); 278-284.
8. Philip B, Xie J, Chandrasekhar A, Abraham J, Varadan V. A novel nanocomposite from multiwalled carbon nanotubes functionalized with a conducting polymer. *Smart mater Struct*, 2004; 13(2); 295.
9. Ai L, Liu Y, Zhang X, Ouyang X, Ge Z. A facile and template-free method for preparation of polythiophene microspheres and their dispersion for waterborne corrosion protection coatings. *Synth Met*, 2014; 191; 41-46.
10. Patil B, Jagadale A, Lokhande C. Synthesis of polythiophene thin films by simple successive ionic layer adsorption and reaction (SILAR) method for supercapacitor application. *Synth Met*, 2012; 162(15); 1400-1405.
11. Zhang H, Hu L, Tu J, Jiao S. Electrochemically assembling of polythiophene film in ionic liquids (ILs) microemulsions and its application in an electrochemical capacitor. *Electrochim Acta*, 2014; 120; 122-127.
12. Ma G, Liang X, Li L, Qiao R, Jiang D, Ding Y, et al. Cu-doped zinc oxide and its polythiophene composites: Preparation and antibacterial properties. *Chemosphere*, 2014; 100; 146-151.
13. Xu M, Zhang J, Wang S, Guo X, Xia H, Wang Y, et al. Gas sensing properties of SnO_2 hollow spheres/polythiophene inorganic-organic hybrids. *Sens Actuators B*, 2010; 146(1); 8-13.
14. Bhagiyalakshmi M, Hemalatha P, Palanichamy M, Jang HT. Adsorption, regeneration and interaction of CO_2 with a polythiophene-carbon mesocomposite. *Colloids Sur A*, 2011; 374(1); 48-53.
15. Guo X, Kang Y, Yang T, Wang S. Low-temperature NO_2 sensors based on polythiophene/ WO_3 organic-inorganic hybrids. *Trans Nonferrous Met Soc. China*, 2012; 22(2); 380-385.
16. Kymakis E, Amaratunga G. Single-wall carbon nanotube/conjugated polymer photovoltaic devices. *Appl Phys Lett*, 2002; 80(1); 112-114.
17. Liu J, Kadnikova E, Liu Y, McGehee M, Fréchet J. Polythiophene containing thermally removable solubilizing groups enhances the interface and the performance of polymer-titania hybrid solar cells. *J Am Chem Soc*, 2004;

- 126(31); 9486-9487.
18. Jang W, Yun J, Kim H, Lee Y. Preparation and characteristics of conducting polymer-coated multiwalled carbon nanotubes for a gas sensor. *Carb Lett*, 2011; 12(3); 162-166.
 19. Whitby R, Korobeinyk A, Mikhailovsky S, Fukuda T, Maekawa T. Morphological effects of single-layer graphene oxide in the formation of covalently bonded polypyrrole composites using intermediate diisocyanate chemistry. *J Nanopart Res*, 2011; 13(10); 4829-4837.
 20. Xiang C, Jiang D, Zou Y, Chu H, Qiu S, Zhang H, et al. Ammonia sensor based on polypyrrole-graphene nanocomposite decorated with titania nanoparticles. *Ceram Int*, 2015; 41(5); 6432-6438.
 21. An K, Jeong S, Hwang H, Lee Y. Enhanced sensitivity of a gas sensor incorporating single-walled carbon nanotube-polypyrrole nanocomposites. *Adv Mater*, 2004; 16(12); 1005-1009.
 22. Singh S, Yadav B, Singh A, Dwivedi P. Synthesis of nanostructured iron-antimonate and its application as liquefied petroleum gas sensor. *Adv Mater Lett*. 2012; 3; 154-160.
 23. Barkade S, Pinjari D, Nakate U, Singh A, Gogate P, Naik J, et al. Ultrasound assisted synthesis of polythiophene/SnO₂ hybrid nanolatex particles for LPG sensing. *Chem Eng Process*, 2013; 74; 115-123.
 24. Venkatesan R, Cindrella L. Semiconducting composite of chalcone-bridged polythiophene and titania, its ammonia vapor sensing property. *Mater Sci Semicond Process*, 2015; 34; 126-137.
 25. Yun J, Im J, Kim H, Lee Y. Effect of oxyfluorination on gas sensing behavior of polyaniline-coated multi-walled carbon nanotubes. *Appl Surf Sci*, 2012; 258(8); 3462-3468.
 26. Ngo C, Le Q, Ngo T, Nguyen D, Vu M. Surface modification and functionalization of carbon nanotube with some organic compounds. *Adv Nat Sci: Nanosci Nanotechnol*, 2013; 4(3); 035017.
 27. Bachhav S, Patil D. Study of Polypyrrole-Coated MWCNT Nanocomposites for Ammonia Sensing at Room Temperature. *J Mater Sci Chem Eng*, 2015; 3(10); 30.
 28. Fu C, Zhou H, Liu R, Huang Z, Chen J, Kuang Y. Supercapacitor based on electropolymerized polythiophene and multi-walled carbon nanotubes composites. *Mater Chem Phys*, 2012; 132(2); 596-600.
 29. Zhang B, Xu Y, Zheng Y, Dai L, Zhang M, Yang J, et al. A facile synthesis of polypyrrole/carbon nanotube composites with ultrathin, uniform and thickness-tunable polypyrrole shells. *Nanoscale Res Lett*, 2011; 6(1); 1-9.
 30. Guo H, Zhu H, Lin H, Zhang J, Yu L. Synthesis and characterization of multi-walled carbon nanotube/polythiophene composites. *J Dispersion Sci Technol*, 2008; 29(5); 706-710.
 31. Dresselhaus M, Dresselhaus G, Saito R, Jorio A. Raman spectroscopy of carbon nanotubes. *Phys Rep*, 2005; 409(2); 47-99.
 32. Cochet M, Louarn G, Quillard S, Buisson J, Lefrant S. Theoretical and experimental vibrational study of emeraldine in salt form. Part II. *J Raman Spectrosc*, 2000; 31(12); 1041-1049.
 33. Karim M, Lee C, Lee M. Synthesis and characterization of conducting polythiophene/carbon nanotubes composites. *J Polym Sci Part A: Polym Chem*, 2006; 44(18); 5283-5290.
 34. Liu P, Wang X, Li H. Preparation of carboxylated carbon nanotubes/polypyrrole composite hollow microspheres via chemical oxidative interfacial polymerization and their electrochemical performance. *Synth Met*, 2013; 181; 72-78.
 35. Zhao J, Xie Y, Le Z, Yu J, Gao Y, Zhong R, et al. Preparation and characterization of an electromagnetic material: The graphene nanosheet/polythiophene composite. *Synth Met*, 2013; 181; 110-116.
 36. Zabihi O, Khodabandeh A, Mostafavi S. Preparation, optimization and thermal characterization of a novel conductive thermoset nanocomposite containing polythiophene nanoparticles using dynamic thermal analysis. *Polym Degrad Stab*, 2012; 97(1); 3-13.
 37. Gnanakan S, Rajasekhar M, Subramania A. Synthesis of polythiophene nanoparticles by surfactant-assisted dilute polymerization method for high performance redox supercapacitors. *Int J Electrochem Sci*, 2009; 4; 1289-1301.
 38. Wang L, Jia X, Wang D, Zhu G, Li J. Preparation and thermoelectric properties of polythiophene/multiwalled carbon nanotube composites. *Synth Met*, 2013; 181; 79-85.
 39. Karim M, Yeum J, Lee M, Lim K. Synthesis of conducting polythiophene composites with multi-walled carbon nanotube by the γ -radiolysis polymerization method. *Mater Chem Phys*, 2008; 112(3); 779-782.
 40. Van Hieu N, Thuy L, Chien N. Highly sensitive thin film NH₃ gas sensor operating at room temperature based on SnO₂/MWCNTs composite. *Sens Actuators B*, 2008; 129(2); 888-895.
 41. Yu Y, Ouyang C, Gao Y, Si Z, Chen W, Wang Z, et al. Synthesis and characterization of carbon nanotube/polypyrrole core-shell nanocomposites via in situ inverse microemulsion. *J Polym Sci, Part A: Polym Chem*, 2005; 43(23); 6105-6115.
 42. Zhang X, Zhang J, Wang R, Zhu T, Liu Z. Surfactant-directed polypyrrole/cnt nanocables: Synthesis, characterization, and enhanced electrical properties. *ChemPhysChem*, 2004; 5(7); 998-1002.
 43. Chen Y, Li Y, Wang H, Yang M. Gas sensitivity of a composite of multi-walled carbon nanotubes and polypyrrole prepared by vapor phase polymerization. *Carbon*, 2007; 45(2); 357-363.
 44. Sahoo N, Jung Y, So H, Cho J. Polypyrrole coated carbon nanotubes: synthesis, characterization, and enhanced electrical properties. *Synth Met*, 2007; 157(8); 374-379.
 45. Lokhande C, Gondkar P, Mane R, Shinde V, Han S. CBD grown ZnO-based gas sensors and dye-sensitized solar cells. *J Alloys Compd*, 2009; 475(1); 304-311.